**Bofeng Shang**
School of Energy and Power Engineering,
Huazhong University of Science and Technology,
Wuhan 430074, China
e-mail: shangbofeng_hust@163.com

**Xingjian Yu**
School of Energy and Power Engineering,
Huazhong University of Science and Technology,
Wuhan 430074, China
e-mail: yuxingjian_hust@163.com

**Huai Zheng**
School of Energy and Power Engineering,
Huazhong University of Science and Technology,
Wuhan 430074, China
e-mail: huai_zheng@whu.edu.cn

**Bin Xie**
School of Energy and Power Engineering,
Huazhong University of Science and Technology,
Wuhan 430074, China
e-mail: xiebinhust@163.com

**Qi Chen**
School of Energy and Power Engineering,
Huazhong University of Science and Technology,
Wuhan 430074, China
e-mail: cooche@hust.edu.cn

**Xiaobing Luo**[1]
School of Energy and Power Engineering,
Huazhong University of Science and Technology,
Wuhan 430074, China
e-mail: luoxb@hust.edu.cn

# Numerical and Experimental Study on the Transferred Volume in Phosphor Dip-Transfer Coating Process of Light-Emitting Diodes Packaging

*The phosphor dip-transfer coating method is simple and flexible for transferring a pre-analyzed volume of phosphor gel, which can be beneficial to the high angular color uniformity (ACU) of white light-emitting diodes (LEDs). The crux of this method is the volume control of the phosphor gel; however, the critical factors which influence the volume control remain unrevealed. In this paper, we concentrate on investigating the transferred volume in terms of three parameters: withdrawal speed, post radius, and dipping depth. Numerical simulations were carried out utilizing the volume of fluid (VOF) model combined with the dynamic mesh model. The experiments were also conducted on an optical platform equipped with a high-speed camera. The simulation results coincide well with the experimental results, with the maximum relative difference within 15%. The results show that the transferred volume increases with the increasing withdrawal speed and remains stable when the speed is greater than 1 mm/s, and it shows a linear relationship with the cube of post radius. And the transferred volume will increase with the dipping depth. Based on the experimental and numerically work, it is concluded that the volume of the pre-analyzed phosphor gel can be precisely obtained.* [DOI: 10.1115/1.4033165]

*Keywords: dip-transfer coating, transferred volume, VOF model*

## 1 Introduction

As green light sources, high-power LEDs have obtained high recognition and been widely applied in various illumination applications [1–4]. The packaging processes especially coating process are of great significance to the performance of LEDs [5,6]. Usually, two kinds of coating methods are widely used in the packaging processes which are direct liquid dispensing and conformal coating [7–9]. However, it becomes inapplicable with very small volume for the liquid behavior cannot be accurately controlled at large driving pressure [10]. In addition, the geometry of the phosphor gel is a big spherical cap by direct liquid dispensing, consequently lead to a low ACU. Recently, Zheng et al. presented a phosphor dip-transfer coating method to realize high ACU for phosphor-converted white LEDs [10,11]. Dip coating is a common method and extensively applied in some industries because of its simplicity and high throughput [12]. The advantage of this technology is well handling very little volume liquid by depositing it on plane and cylindrical surface. The key to this method is the volume control of the phosphor gel, but there is few clear understanding on the critical factors and influence rules toward the phosphor gel volume of dip-transfer process currently.

The related researches are mainly based on experiment [13,14], which leads to a limited significance to the coating process. Lian et al. experimentally analyzed the transferred volume by creating and disconnecting liquid bridges [15]. The liquid bridge disconnected is a representative mechanism for volume transfer from one body to another. Liquid bridges are fluid formed between two or more solid surfaces. The geometry and related forces of liquid bridges have been studied to understand physics involved in microscale solid–liquid interaction [16]. A dynamic behavior of liquid bridges was also investigated [17], but further applications of theoretical or experimental analysis on the liquid bridges have been rarely reported so far.

To capture the geometry changes of the phosphor gel through numerical simulation, the VOF model can be implemented. Zhang showed that numerical simulations of drop formation using the VOF method agreed well with experimental results [18]. Huang et al. used the VOF method to simulate the rupturing of the liquid filament and the subsequent generation of satellite droplets during gravure-offset printing. They comprehensively explained the influence of separation velocity, liquid viscosity, surface tension, gravitational force, and contact angle on ink transfer for gravure-offset printing [19].

In this paper, we created a liquid bridge to study the flow mechanism of the phosphor gel during the dip-transfer process. We numerically and experimentally investigated the effect of three parameters in terms of withdrawal speed, post radius, and dipping depth on the transferred volume of liquid. Based on the experimental and numerically work, a quantitative analysis of these parameters affecting the transferred volume is explicit, and a pre-analyzed volume of phosphor gel can be precisely obtained.

[1]Corresponding author.

Contributed by the Electronic and Photonic Packaging Division of ASME for publication in the JOURNAL OF ELECTRONIC PACKAGING. Manuscript received June 17, 2015; final manuscript received March 15, 2016; published online April 19, 2016. Assoc. Editor: Shi-Wei Ricky Lee.

  

## 2 Phosphor Dip-Transfer Coating Process

The phosphor dip-transfer coating process including two steps: one is from the mixture to the post and the other is from the post to the package. Through our research, we found the parameter effect in the second step is nearly similar with the first step, so we focus on the former process. Figure 1 shows the first process and it includes the following steps:

(1) Dipping the post into the phosphor gel up to a predefined depth, and a meniscus will be formed gradually under the effect of capillary force (Fig. 1(*a*)).
(2) Lifting the post with a speed, $U$, and then a liquid bridge will be created transiently between the post and the mixture (Fig. 1(*b*)).
(3) While the post is drew up with a certain speed, the neck of the liquid bridge became narrow, and there exists a pressure difference between the mixture and the air, which can be determined by Young–Laplace equation

$$\Delta P = \gamma\left(\frac{1}{R_1}+\frac{1}{R_2}\right) \tag{1}$$

where $\gamma$ is the surface tension, $R_1$ and $R_2$ are the principal radius of the meniscus curvature in the width and height directions, respectively (Fig. 1(*c*)).

(4) After the post is lifted from the mixture, the liquid bridge will be disconnected, a very small volume of the phosphor mixture is transferred to the post bottom surface (Fig. 1(*d*)).

From the above analysis, the withdrawal speed, post radius, and dipping depth may affect the transferred volume. Therefore, a physical model should be established to study these factors toward the transferred volume.

## 3 Numerical Model and VOF Numerical Method

Numerical simulations were conducted by finite element method. A precise numerical model is essential to the final simulation accuracy. The VOF model combined with the dynamic mesh model was employed to simulate phosphor dip-transfer coating process. Due to the motion of the post, the normal simulation method cannot be used for the analysis of the process. Dynamic mesh technique, which is generally used to model flows where the shape of the domain changes with time due to motion on the domain boundaries, was utilized to simulate the motion of the post. The update of the volume mesh is handled at each time step based on the new positions of the boundaries. The motion of domain boundary was described by user-defined function.

**3.1 Mathematical Models.** VOF model is on the basis of fluid in the grid cell of volume function $F$ to structure and track free surface each moment. If $F$ equals to one in the grid cell at a moment, it shows that this unit is fluid unit which is all held by the specified fluid; if $F$ equals to zero, this unit is all held by another fluid, it is called for empty unit relative to the former fluid, when $F$ is larger than zero and less than one, this unit is the interface unit which contains two phase materials [20].

(1) Volume function $F$ changes with time following the following equation:

$$\frac{\partial F}{\partial t}+\nabla\cdot(F\mathbf{u})=0 \tag{2}$$

(2) The continuity equation of volume fraction

$$\frac{\partial \alpha_i}{\partial t}+\mathbf{u}\nabla\alpha_i=0 \tag{3}$$

Among them

$$\sum_{i=1}^{n}\alpha_i=1 \tag{4}$$

(3) The velocity vector can be solved by the momentum equation

$$\frac{\partial(\rho\mathbf{u})}{\partial t}+\nabla\cdot(\rho\mathbf{u}\mathbf{u})=-\nabla p+\nabla\left[\mu(\nabla\mathbf{u}+\nabla\mathbf{u}^T)\right]+\rho\mathbf{g}+\mathbf{F}_s \tag{5}$$

Among the formula $\mathbf{F}_s$ is the origin of the momentum equation which is caused by surface tension and wall surface adhering effect

$$\mathbf{F}_s=2\sigma k\alpha_i\nabla\alpha_i \tag{6}$$

Among the formula: $\sigma$ is surface tension constant; $\mathbf{u}$ is velocity vector; $\mu$ is fluid dynamic viscosity; $\alpha_i$ is the volume fraction of the phase; $k$ is surface curvature.

**3.2 Calculation Model and Boundary Conditions.** Figure 2 shows the physical model. A two-dimensional symmetrical model was adopted to simplify the calculation for the model is axisymmetric. Each simulation was performed from a predefined distance $h$ where the post dipped into the phosphor gel. The initial distance and velocity varies from one simulation to another. The bottom, the sidewall, and the post surfaces were set as wall. The top surface was set as pressure-outlet.

For all the simulations presented in this work, the viscosity $\mu$ of phosphor gel was set as 4 Pa · s according to the test results by the viscometer CAP2000, the surface tension of the mixture was set as 0.03 N/m which was measured using pendant drop experiments, and the contact angle was assumed to be static and constant [21] during each simulation at a value of 15 deg by experiment. The withdrawal speed varies from 0.1 mm/s to 4 mm/s, the post radius

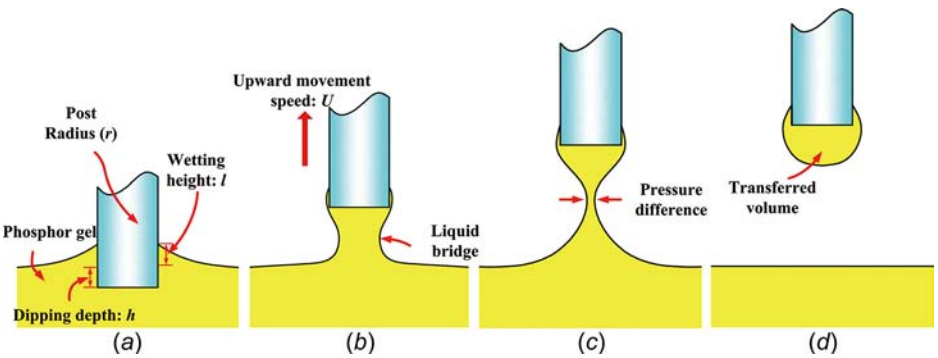


**Fig. 1 Schematics of phosphor dip-transfer coating. (*a*) Dipping the post into the mixture. (*b*)–(*d*) Drawing the post with a predefined speed.**

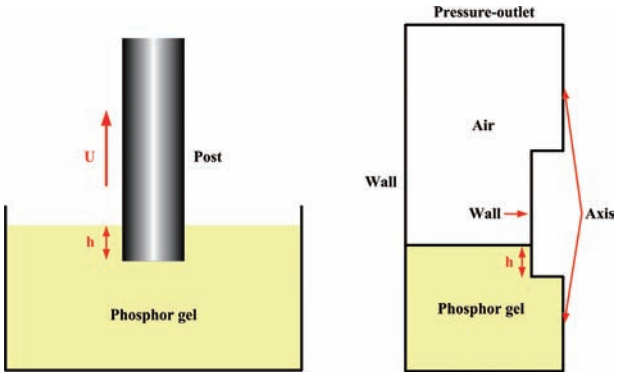


**Fig. 2 Physical model of numerical simulation**

varies from 0.64 mm to 2.1 mm, and the dipping depth of the post varies from 0 mm to 2 mm. The surface tension, gravity, and fluid viscous force were considered in the calculation model. Since the density and viscosity of the gas phase are orders of magnitude smaller than the liquid phase, the effect of the gas phase on the liquid phase is not significant in our numerical simulations. In order to make the simulation more realistic with the coating process, the simulation was divided into two stages: During the first stage, the post was static, the phosphor will automatically wet the post under capillary force, and reach a steady-state finally. During the second stage, the post will be drawn up at a predefined speed to simulate the process of coating.

## 4 Experiments

Figure 3 shows the experimental schematic of the phosphor dip-transfer coating processes. It is noted that the experimental working conditions were the same as those in numerical simulation. The post was connected to an electric motor to realize the vertical movement at a certain velocity. We used the high-speed camera equipped with a microscopic lens to monitor the fluid flow. A light source was utilized to ensure a high brightness illumination in the process of filming. To adjust the depth of the post in phosphor gel, we designed a platform which could realize a micro motion in both horizontal and vertical directions.

The experiments were performed at room temperature (20 °C). As a test material, the silicone–phosphor gel with a concentration of 0.1 g/cm$^3$ was applied in the experiments. The phosphor particles were sufficiently blended with the silicone (Dow Corning OE-6550), phosphor powder was produced by Intematix and the model number is YAG-04 with averaging particle diameter of 13 $\mu$m. The fluid properties, the withdrawal speed, the post radius, and the dipping depth of the post are chosen to accord with those used in the simulations described above.

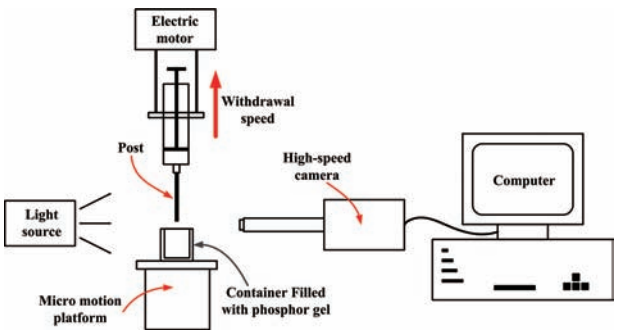


**Fig. 3 Schematic of the experimental setup**

## 5 Results and Discussion

Figure 4 shows the comparison between our numerical simulations and the experimental results at different moments of the dip-transfer process. The figure indicates good agreement between simulation and experiment.

Figure 5 shows the transferred volume varies with the variation of withdrawal speed. When investigated the influence of the post's withdrawal speed, the other conditions were fixed, $d = 1.15$ mm, $h = 0$ mm. Here, $U$ represents the withdrawal speed, $d$ represents post diameter, and $h$ represents dipping depth. The capillary number ($Ca = \mu U/\gamma$, $\gamma$ was the measured surface tension of 0.03 N/m) varied from 0.0133 to 0.5333 as the withdrawal speed increased from 0.1 mm/s to 4 mm/s. The large capillary number (typically larger than $10^{-5}$) represents the increased effects of viscosity on the fluid dynamics [22], which contributes to the increase of the volume adhere to the post. Therefore, the phenomenon that the transferred volume increases with the withdrawal speed can be interpreted by the capillary number [23]. In addition, we observed that the mixture adhering to post sidewalls also contributed to the final volume. In case of a low capillary number of 0.0133 ($U = 0.1$ mm/s), a large portion of mixture adhering to sidewall flew down to a liquid bridge before the end of disconnection. On the contrary, the sidewall mixture flew down after liquid bridge disconnection and contributed to the transferred volume if capillary number is large [22]. However, the transferred volume barely changed once the withdrawal speed is over 1 mm/s, which may stem from the greater withdrawal speed. While the speed is great enough, the liquid bridge will be disconnected soon, and then the volume adhere to the post will barely change.

Figure 6 shows the transferred volume varies with the variation of the cube of post radius while the other conditions were also

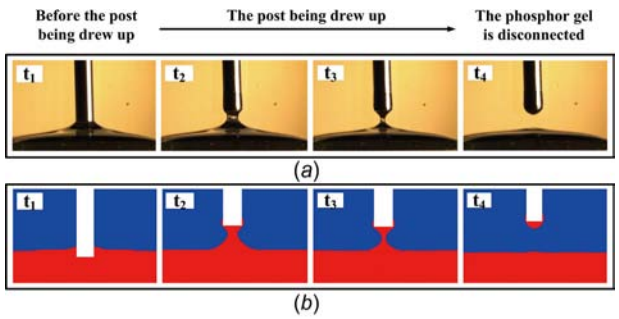


**Fig. 4 The phosphor gel geometry changes over time during dip-transfer process. (*a*) Experiment results and (*b*) numerical simulation results.**

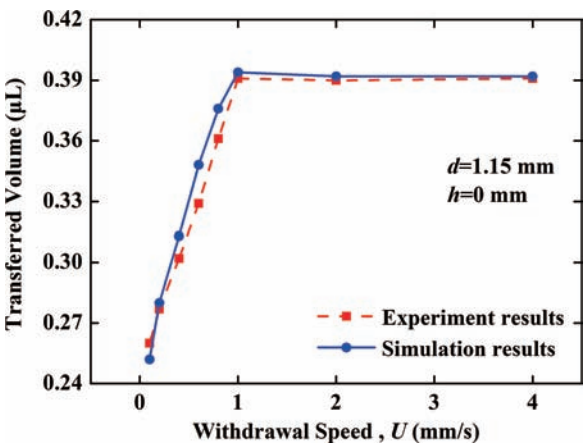


**Fig. 5 The transferred volume varies with the variation of withdrawal speed**

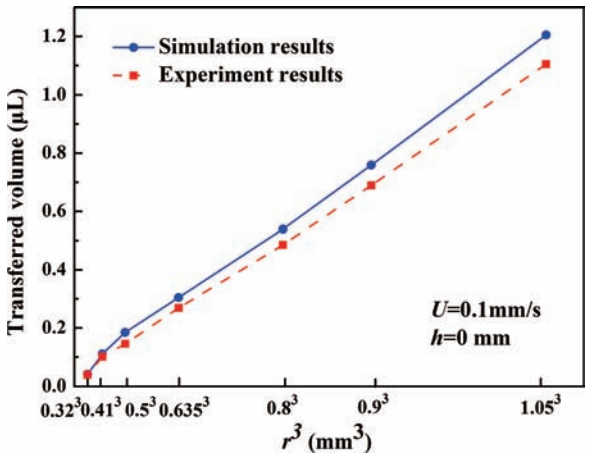


**Fig. 6 The transferred volume varies with the variation of $r^3$**

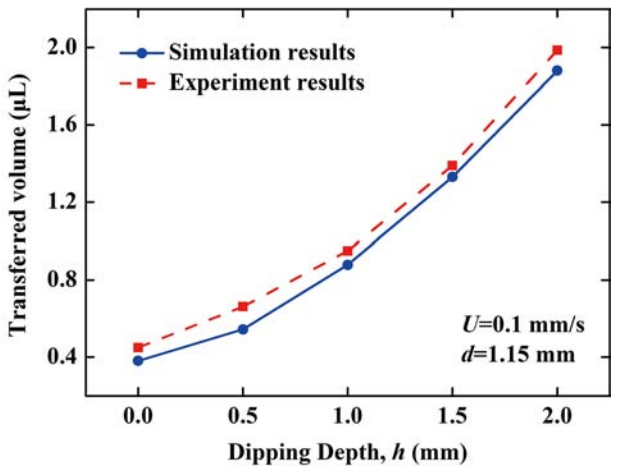


**Fig. 7 The transferred volume varies with the variation of dipping depth**

fixed, $U = 0.1$ mm/s, $h = 0$ mm. The transferred volume (1.105 $\mu$L) of 2.1 mm post was 28 times larger than that (0.0392 $\mu$L) of 0.64 mm post. Greater size of the post can provide more kinetic energy to the mixture to overcome the viscosity force and adhere to the post. The transferred volume versus $r^3$ was plotted in Fig. 6 and it can be seen that the transferred volume clearly depends on a linear relationship with $r^3$. In terms of geometric relationships, the relationship between radius and volume is cubic. Therefore, it can clearly explain why the transferred volume represents a linear relationship with $r^3$.

Figure 7 shows the transferred volume varies with the variation of dipping depth, the other conditions were fixed, $U = 0.1$ mm/s, $d = 1.15$ mm. The transferred volume varies from 0.45 $\mu$L to 1.986 $\mu$L and the dipping depth varies from 0 mm to 2 mm. The results show that the transferred volume increase with the dipping depth and the slope is slightly increased. The increase of the dipping depth contributes to the kinetic energy transfer from the post to the phosphor gel, then overcoming the viscosity force and adhering to the post. And it also contributes to a larger portion of mixture adhering to sidewall, then the slope will gradually increase.

## 6 Conclusion

In summary, we numerically and experimentally analyzed the influence of the post radius, withdrawal speed and dipping depth on the transferred volume in the phosphor dip-transfer coating process. The simulation results coincide well with the experimental results, with the maximum relative difference within 15%. The results show that the transferred volume will increase with the withdrawal speed but tend to be stable while the speed is over 1 mm/s. The post radius is the major factors for the volume representing a linear relationship with $r^3$, and the volume will increase with the dipping depth. Through these investigations, a clear understanding on how each factor influences the volume of the phosphor gel in the dip-transfer coating process can be acquired. Thus, the pre-analyzed volume of phosphor gel can be obtained precisely, which can be beneficial for the industrial community to manufacture LEDs with high performance.


## Acknowledgment

The authors would like to acknowledge the financial support partly by National Science Foundation of China (Nos. 51376070 and 51576078), and partly by 973 Project of The Ministry of Science and Technology of China (No. 2011CB013105).


## Nomenclature

$F$ = volume function
$h$ = dipping depth (mm)
$k$ = surface curvature
$r$ = post radius (mm)
$R_1$ = the principal radius of the meniscus curvature in the width direction (mm)
$R_2$ = the principal radius of the meniscus curvature in the height directions (mm)
$\mathbf{u}$ = velocity vector
$U$ = withdrawal speed (mm/s)
$\alpha_i$ = volume fraction of the phase
$\gamma$ = surface tension (N/m)
$\mu$ = fluid dynamic viscosity (Pa · s)
$\sigma$ = surface tension constant

## References


[1] Liu, S., and Luo, X. B., 2011, *LED Packaging for Lighting Applications: Design, Manufacturing, and Testing*, Wiley, Hoboken, NJ.
[2] Yuan, C., Xie, B., Huang, M. Y., Wu, R. K., and Luo, X. B., 2016, "Thermal Conductivity Enhancement of Platelets Aligned Composites With Volume Fraction From 10% to 20%," Int. J. Heat Mass Transfer, **94**, pp. 20–28.
[3] Petroski, J., 2014, "Advanced Natural Convection Cooling Designs for Light-Emitting Diode Bulb Systems," ASME J. Electron. Packag., **136**(4), p. 041005.
[4] Yuan, C., Li, L., Duan, B., Xie, B., Zhu, Y. M., and Luo, X. B., 2016, "Locally Reinforced Polymer-Based Composites for Efficient Heat Dissipation of Local Heat Source," Int. J. Therm. Sci., **102**, pp. 202–209.
[5] Lin, Y. C., You, J. P., Tran, N. T., He, Y. Z., and Shi, F. G., 2011, "Packaging of Phosphor Based High Power White LEDs: Effects of Phosphor Concentration and Packaging Configuration," ASME J. Electron. Packag., **133**(1), p. 011009.
[6] You, J. P., Lin, Y. H., Tran, N. T., and Shi, F. G., 2010, "Phosphor Concentration Effects on Optothermal Characteristics of Phosphor Converted White Light-Emitting Diodes," ASME J. Electron. Packag., **132**(3), p. 031010.
[7] Zheng, H., Ma, J. L., and Luo, X. B., 2013, "Conformal Phosphor Distribution for White Lighting Emitting Diode Packaging by Conventional Dispensing Coating Method With Structure Control," IEEE Trans. Compon., Packag., Manuf. Technol., **3**(3), pp. 417–421.
[8] Huang, H. T., Tsai, C. C., and Huang, Y. P., 2010, "Conformal Phosphor Coating Using Pulsed Spray to Reduce Color Deviation of White LEDs," Opt. Express, **18**(102), pp. A201–A206.
[9] Zheng, H., Wang, Y. M., Fu, X., Liu, S., and Luo, X. B., 2013, "Conformal Phosphor Coating for Phosphor-Converted White LEDs on Basis of Dispensing Process," 14th International Conference on Electronic Packaging Technology (ICEPT), Dalian, China, Aug. 11–14, pp. 1138–1141.
[10] Zheng, H., Liu, S., and Luo, X. B., 2013, "Enhancing Angular Color Uniformity of Phosphor-Converted White Light-Emitting Diodes by Phosphor Dip-Transfer Coating," IEEE J. Lightwave Technol., **31**(12), pp. 1987–1993.
[11] Zheng, H., Wang, Y. M., Li, L., Fu, X., Zou, Y., and Luo, X. B., 2013, "Dip-Transfer Phosphor Coating on Designed Substrate Structure for High Angular Color Uniformity of White Light Emitting Diodes With Conventional Chips," Opt. Express, **21**(S6), pp. 933–941.
[12] Darhuber, A. A., Troian, S. M., Davis, J. M., Miller, S. M., and Wagner, S., 2000, "Selective Dip-Transfer Coating of Chemically Micropatterned Surfaces," J. Appl. Phys., **88**(9), pp. 5119–5126.

[13] Vega, E. J., Montanero, J. M., Herrada, M. A., and Ferrera, C., 2014, "Dynamics of an Axisymmetric Liquid Bridge Close to the Minimum-Volume Stability Limit," Phys. Rev. E, **90**(1), p. 013015.
[14] Kumar, S., 2015, "Liquid Transfer in Printing Processes: Liquid Bridges With Moving Contact Lines," Annu. Rev. Fluid Mech., **47**(1), pp. 67–94.
[15] Lian, G., Thornton, C., and Adams, M. J., 1993, "A Theoretical Study of the Liquid Bridge Forces Between Two Rigid Spherical Bodies," J. Colloid Interface Sci., **161**(1), pp. 138–147.
[16] Pitois, O., Moucheront, P., and Chateau, X., 2000, "Liquid Bridge Between Two Moving Spheres: An Experimental Study of Viscosity Effects," J. Colloid Interface Sci., **231**(1), pp. 26–31.
[17] Gao, S. Q., Jin, L., Du, J. Q., and Liu, H. P., 2011, "The Liquid-Bridge With Large Gap in Micro Structural Systems," J. Mod. Phys., **2**(5), pp. 404–415.
[18] Zhang, X., 1999, "Dynamics of Drop Formation in Viscous Flows," Chem. Eng. Sci., **54**(12), pp. 1759–1774.
[19] Huang, W. X., Lee, S. H., Sung, H. J., Lee, T. M., and Kim, D. S., 2008, "Simulation of Liquid Transfer Between Separating Walls for Modeling Micro-Gravure-Offset Printing," Int. J. Heat Fluid Flow, **29**(5), pp. 1436–1446.
[20] Liu, X. Y., Chen, W., Liu, L. J., and Liu, D. W., 2013, "The Numerical Simulation of Oil-Water Two Phase Flow in Horizontal Pipeline Based on the VOF Model," 7th International Symposium on Multiphase Flow, Heat Mass Transfer and Energy Conversion (ISMF 2012), Xi'an, China, Oct. 26–30, Vol. 1547(1), pp. 741–745.
[21] Caviezel, D., Narayanan, C., and Lakehal, D., 2008, "Adherence and Bouncing of Liquid Droplets Impacting on Dry Surfaces," Microfluid. Nanofluid., **5**(4), pp. 469–478.
[22] Jang, Y. H., Lee, K., and Kim, Y. K., 2012, "Controlled Volume Transfer and Lens Shape Formation by Liquid Bridge Disconnection," Appl. Phys. Lett., **100**(21), p. 214103.
[23] Krechetnikov, R., and Homsy, G. M., 2005, "Experimental Study of Substrate Roughness and Surfactant Effects on the Landau-Levich Law," Phys. Fluids, **17**(10), p. 102108.